

Online Supplemental Information

The additional information presented in the Online Supplement includes:

A. Three figures of additional results to extend data reported in the main manuscript.

1. Supplement Figure S1 (related to Figure 4 in main manuscript)

Plot of increases in body weight of individual mice recorded weekly from week 15 to week 48.

Comparisons between the two groups *Ano2*^{+/+} vs. *Ano2*^{+/-} confirm the greater increase in weight of the heterozygotes.

2. Supplement Figure S2 (related to Figure 5 in the main manuscript)

Data extend the information on metabolic changes in heterozygotes (*Ano2*^{+/-}) and littermate controls (*Ano2*^{+/+}) reported in Figure 5. The respiratory exchange ratio and sleep time were not significantly different between the two groups.

3. Supplement Figure S3 (related to Figure 3 and 4 in the main text)

The results in the main text report mRNA expression of *Ano1*, *Ano2*, *CCK1R* and *CCK2R* and the CCK-induced current all in nodose ganglia and nodose neurons. This supplemental Figure S3 reports similar data on DRG ganglia and neurons in contrast to NG. The values in DRG are significantly lower than those in NG. The results support the likelihood that the phenotype of the *TMEM16B* heterozygote KO may reflect a more prominent suppression of CCK activation of vagal nodose ganglia afferents than DRG afferents.

B. Two additional fluorescence Figures S4 & S5 (that complement Figure 3 in the main text):

1. Figure S4 confirms decreased fluorescence of *TMEM16A* and *B* and preserved nuclear staining with DAPI in a section of NG from a mouse on HFD.

2. Figure S5 confirms the *TMEM16B* expression in nodose neurons in culture and localization of *TMEM16B* on the cytoplasmic membrane of cultured neurons.

C. Three Tables:

1. Table S1 provides additional data and results of ANOVA contrasting metabolic responses in *Ano2*^{+/-} vs. *Ano2*^{+/+} mice.

2. Table S2 provides a list of key resources that were used for all materials and animals.

3. Table S3 includes selected primer sequences.

SUPPLEMENTAL INFORMATION

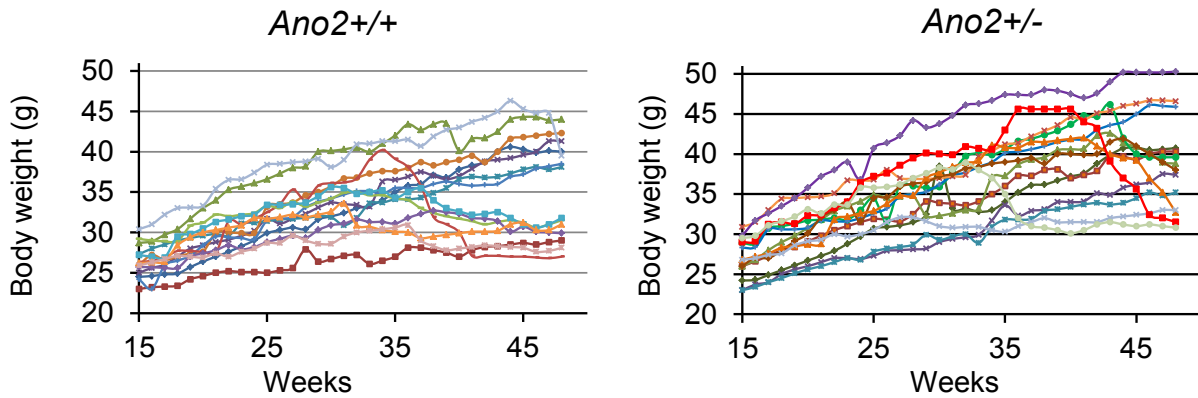


Figure S1. Plot of individual mice body weight up to 48 weeks. Related to Figure 4.

Body weights of control (*Ano2*^{+/+}) and *Nav1.8Cre;Ano2*^{fl/wt} (*Ano2*^{+/-}) mice. The weight increase in *Ano2*^{+/-} mice (n=14) was significantly greater than the wild type controls (*Ano2*^{+/+}; n=14). In a few mice, body weight declined abruptly toward the end of the follow-up period without any obvious explanation. In those mice, the maximal weight attained was included in the calculation of the group means in figure 4B.

Each dot represents a weekly weight and each line connects the weekly weights of each mouse.

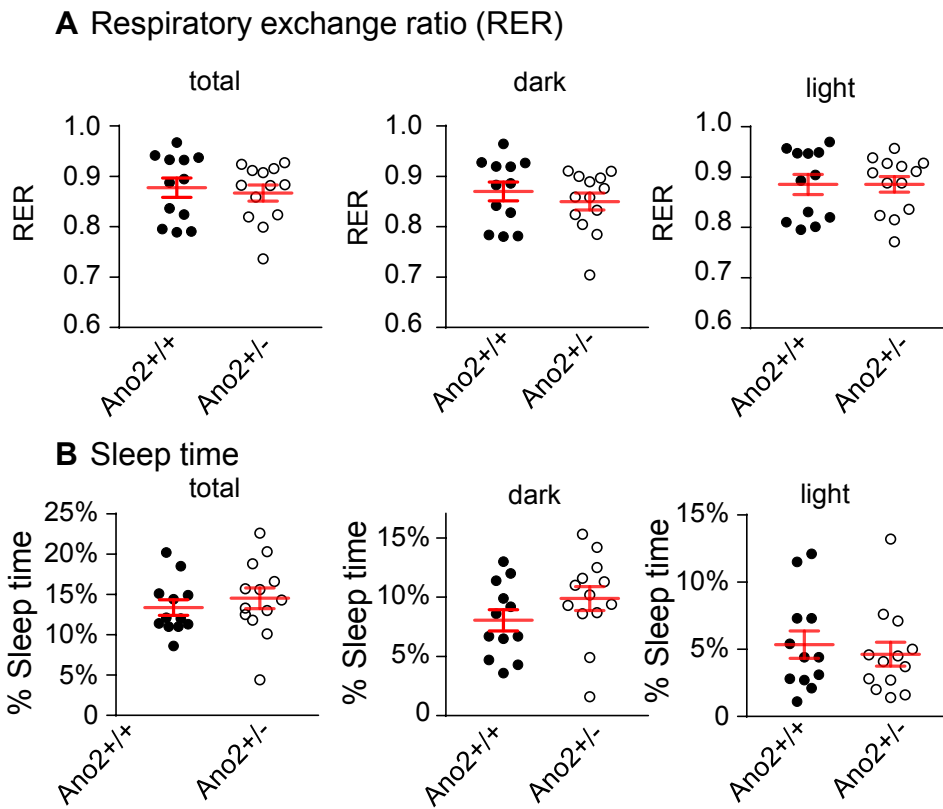


Figure S2. Changes in respiratory exchange ratio and sleep time in control (*Ano2*^{+/+}) vs *Nav1.8* *Cre*;*Ano2*^{fl/wt} (*Ano2*^{+/-}) mice

A. The respiratory exchange ratio (RER) in control vs. *Ano2*^{+/-} mice is 0.88 ± 0.02 vs. 0.87 ± 0.02 for 24 hours total RER (left panel), 0.89 ± 0.02 vs. 0.89 ± 0.02 in light phase (right panel) and 0.87 ± 0.02 vs. 0.85 ± 0.02 in dark phase (middle panel; $p > 0.05$ for all comparisons).

B. The percentile sleep time of control vs. *Ano2*^{+/-} mice is $13.4 \pm 1.0\%$ vs. $14.5 \pm 1.3\%$ of 24 hours total seep time (left panel), $5.4 \pm 1.0\%$ vs. $4.6 \pm 0.9\%$ at light phase (right panel) and $8.1 \pm 0.9\%$ vs. $9.9 \pm 1.0\%$ at dark phase (middle panel; $p > 0.05$ for all comparisons).

Data are presented as means \pm s.e.m., unpaired two-tailed student's t test, each data point represents one individual mouse.

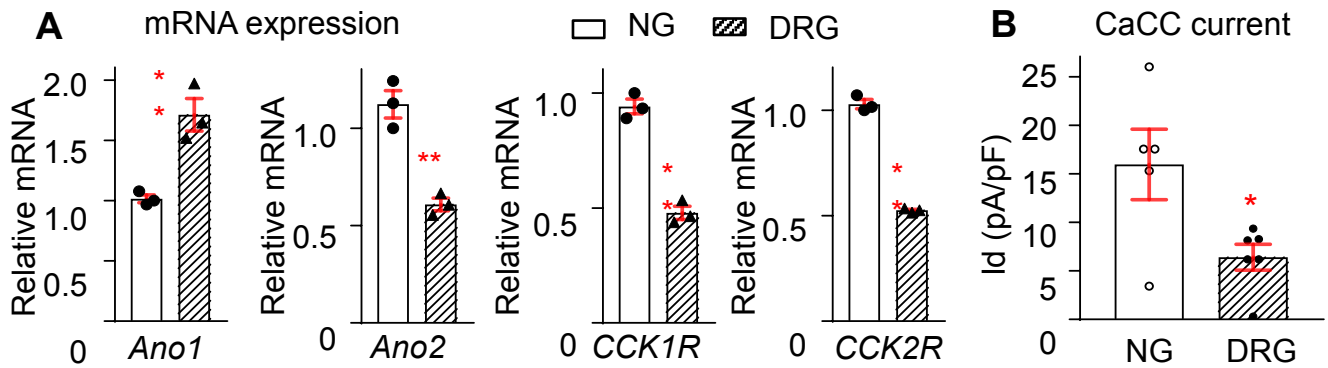


Figure S3. Expression of *Ano2*, *CCK1* and *CCK2* receptors are lower in DRG compared to NG.

A. The relative mRNA levels in NG (open bars) vs. DRG (shaded bars) are 1.02 ± 0.03 vs. 1.71 ± 0.13 for *Ano1*; 1.12 ± 0.07 vs. 0.61 ± 0.03 for *Ano2*; 0.94 ± 0.03 vs. 0.48 ± 0.03 for *CCK1R*; and 1.03 ± 0.02 vs. 0.53 ± 0.01 for *CCK2R*. ** $p < 0.01$, each data point represents two ganglia from one mouse. **B.** The CCK-induced CaCC currents that are inhibited by 300 μM NFA in nodose (NG) vs. DRG neurons are 15.9 ± 3.6 vs. 6.4 ± 1.3 pA/pF. * $p < 0.05$, each data point represents one neuron (from 4 nodose and 4 DRG ganglia obtained from 2 mice).

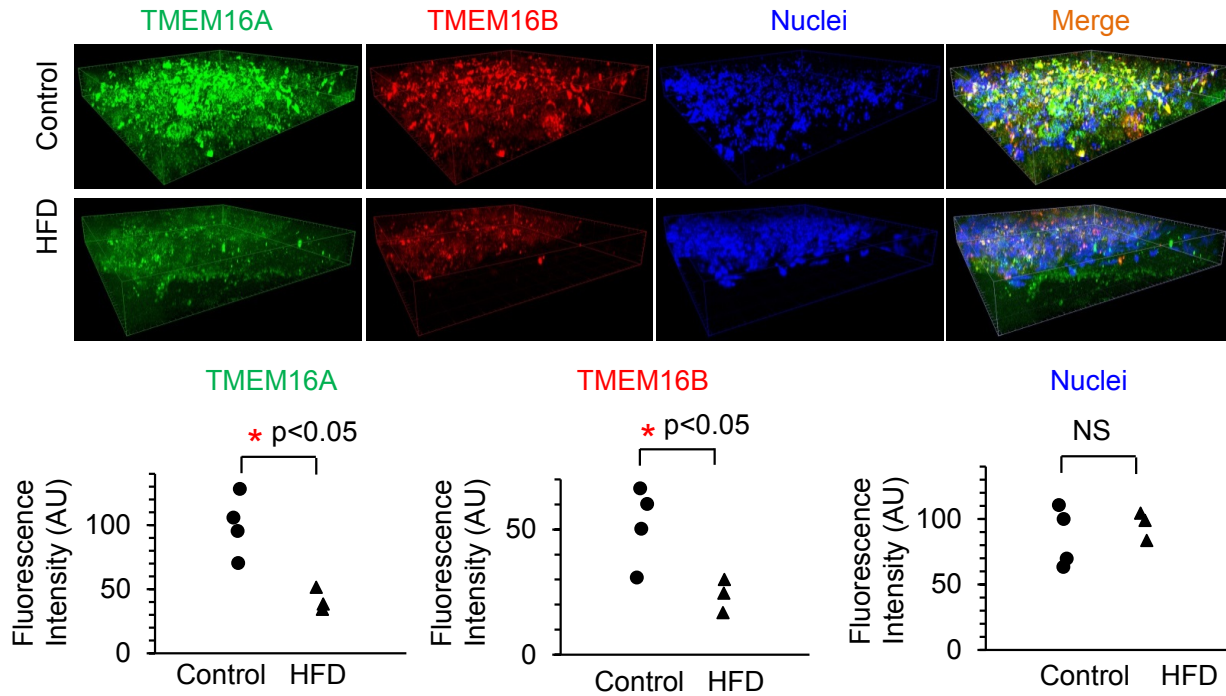
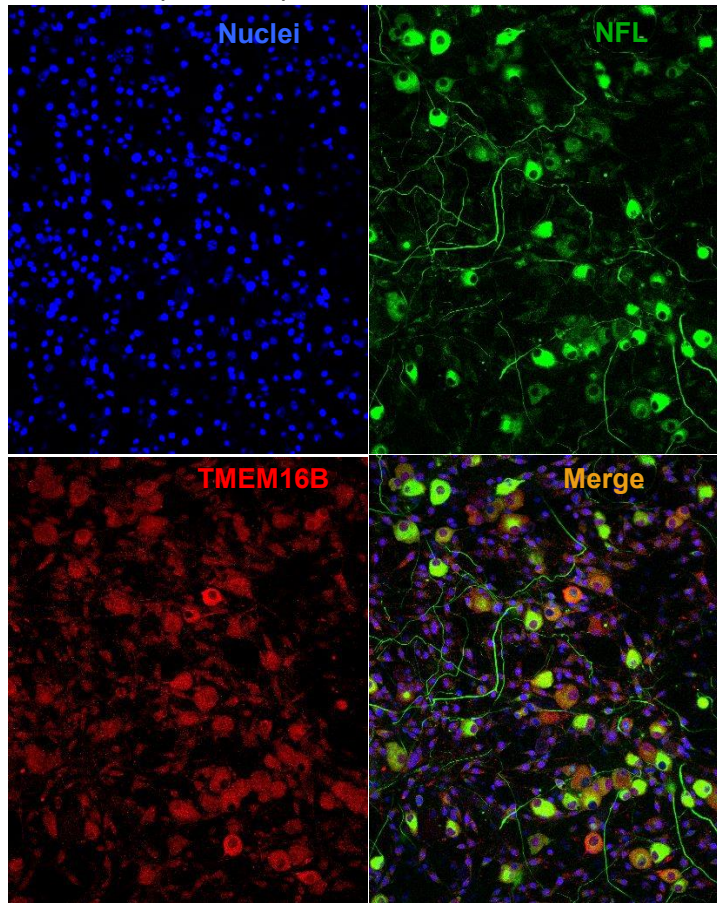


Figure S4. Expression of TMEM16A and B is lower in nodose neurons from mice fed HFD.

A different slice from Figure 3D shows that fluorescence intensity of TMEM16A (green) and B (red) detected by immunohistochemistry are lower in nodose neurons from mice fed a HFD. The values in the graphs show that the quantification of their fluorescence intensity are the same as those shown in **Figure 3** in the main manuscript. The asterisks (*) indicate statistically significant differences. The nuclei (blue) dyed by DAPI shows no difference in fluorescence intensity, suggesting a comparable cell number in nodose ganglia from both groups of mice.

A TMEM16B protein expression in nodose neurons



B TMEM16B expression on the membrane

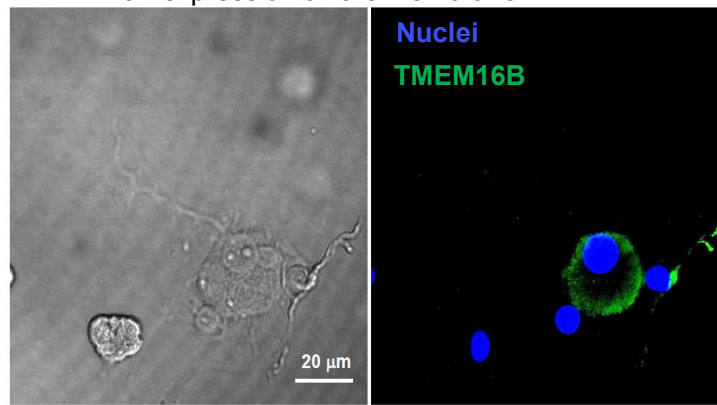


Figure S5. Expression of TMEM16B protein in nodose neurons.

A. DAPI fluorescence of nuclei (blue) and TMEM16B protein stained with anti-Ano2 antibody (red fluorescence) in cultured nodose neurons, which are also labeled by neurofilament light chain (NFL, green).

B. TMEM16B is expressed on the cytoplasmic membrane of the cultured nodose neuron.

Table S1. *Nav1.8Cre;Ano2^{fl/wt}* (*Ano2*^{+/-}) and littermate control (*Ano2*^{+/+}) mice

Measurement	<i>Ano2</i> ^{+/+} mice	<i>Ano2</i> ^{+/-} mice
Baseline 24-hour food intake		
Baseline 24-hour food intake light phase (g)	1.08±0.20	0.75±0.08
Baseline 24-hour food intake dark phase (g)	1.88±0.14	1.84±0.09
Energy expenditure		
Energy expenditure light phase (Kcal/g)	0.090±0.003	0.083±0.002
Energy expenditure dark phase (Kcal/g)	0.110±0.004	0.103±0.003
Locomotor activity light phase count (×10 ⁴)	2.20±0.19	1.61±0.11*
Locomotor activity dark phase count (×10 ⁴)	4.73±0.49	4.04±0.40
Glucose tolerance test (glucose level after 2 mg/g body weight glucose injection) (mg/dl)		
before	136.0±11.1	124.3±12.3
30 min	459.0±37.6	390.1±35.9
60 min	314.9±36.8	235.6±20.2
120 min	171.2±20.8	140.8±9.5
Insulin tolerance test (glucose level after 0.75×10⁻³ U/g body weight insulin injection) (mg/dl)		
before	206.6±9.2	185.9±6.7
15 min	177.3±13.0	170.7±10.8
60 min	109.0±15.3	103.3±11.1
120 min	110.8±10.7	110.0±10.0

Data are presented as means ± s.e.m.; * p<0.05 indicates significant difference between *Ano2*^{+/+} and *Ano2*^{+/-} by unpaired two-tailed student's t test, and † indicates significant differences between *Ano2*^{+/+} and *Ano2*^{+/-} by ANOVA for cumulative 24 hours changes of energy expenditure, locomotor activity, and for glucose tolerance levels over a period of 120 minutes.

There were no significant difference in respiratory exchange ratios or sleep time between *Ano2*^{+/+} and *Ano2*^{+/-} mice (data shown in Supplemental Figure S2).

Table S2. Key resources that were used for all materials and animals

REAGENT or RESOURCE	SOURCE	IDENTIFIER
Antibodies		
Goat polyclonal anti-Ano1	Santa Cruz Biotechnology	Cat # sc-69343, lot # E2714
Rabbit polyclonal anti-Ano2	Santa Cruz Biotechnology	Cat # sc-292004, lot # E2813
donkey anti-goat IgG-FITC	Santa Cruz Biotechnology	Cat# sc-2024
mouse anti-rabbit IgG-TR	Santa Cruz Biotechnology	Cat# sc-3917
Virus Strains		
ANO2 shRNA (m) Lentiviral Particles	Santa Cruz Biotechnology	SC-154400-V
Rodent Diet		
NIH-31 Modified Open Formula Mouse/Rat sterilizable diet	ENVIGO	Cat# 7913
Rodent Diet with 60% kcal% fat	Research Diets INC.	Cat# D12492
Rodent Diet with 45%kcal% fat	Research Diets INC.	Cat# D12451
Chemicals, Peptides and Recombinant Proteins		
(Tyr[S03H]27)Cholecystokinin fragment 26-33 Amide	Sigma-Aldrich	Cat# C2175
CCK Octapeptide, sulfated	Tocris Bioscience	Cat#1166
Molecular Probes™ Fluo-4, AM	Invitrogen Molecular Probes	Cat# 10378062
Pluronic™ F-127	Invitrogen Molecular Probes	Cat# P6867
T16A_{inh-A01}	Sigma-Aldrich	Cat# 613551
Niflumic Acid	Sigma-Aldrich	Cat# N0630
DiI (1,1'-Diocadecyl-3,3,3',3'-tetramethylindocarbocyanine perchlorate)	Molecular Probes	Cat# D282
TRIzol reagent	Life Technologies	Cat# 15596018

DNA-free™ DNA Removal Kit	Ambion	Cat# AM1906
RNeasy Micro Kit	Qiagen	Cat# 74004
AffinityScript QPCR cDNA Synthesis Kit	Agilent Technologies	Cat# 600559
Brilliant II SYBR Green qPCR Master Mix	Agilent Technologies	Cat# 600828
Vectashield Mounting Medium	Vector Laboratories	Cat# H-1500

Experimental Models: Organisms/Strains

Mouse: C57BL/6	The Jackson Laboratory	Stock Number 000664
Mouse: <i>Ano2</i>^{fl/fl}	Dr. Thomas J Jentsch's lab	N/A
Mouse: <i>Nav1.8Cre</i>	Dr. John N. Wood's lab	N/A
Rat: Wistar	Charles River	

Software and Algorithms

MetaMorph 6.1.3	Molecular Devices	N/A
pCLAMP 8	Molecular Devices	N/A
Clamfit 9	Molecular Devices	N/A
Microsoft Excel 2010	Microsoft	N/A
MAXCHELATOR	Stanford University	N/A
GraphPad Prism 7	GraphPad Software	N/A
SYSTAT	SYSTAT Software	N/A
Spike2	CED	N/A
SigmaPlot 10	SYSTAT Software	N/A

Other

NanoDrop 1000	Thermo Scientific	
Model 7000 real-time PCR system	ABI	
Flaming/Brown Micropipette Puller	Sutter Instrument	Model P-97
Comprehensive Lab Animal Monitoring System	Columbus Instruments	
Nuclear Magnetic Resonance	Bruker Minispec	LF50

(NMR)		
glucose meter	Abbott	CFGS293-M1652
Axopatch 200B Amplifier	Axon Instrument	
Microforge	Narishige	MF830
Digidata 1322A Digitizer	Axon Instrument	
Inverted Microscope	Nikon	Eclipse TE-200
RSC-200 rapid solution changer	Bio-Logic Science Instruments	

Table S3. Primer sequences used for real-time PCR

Target Gene Fragment	Genbank Accession	Primer Sequences
<i>Ano1</i> 127 bp	NM_178642	Forward: 5'-GAA AAC CAT CAA CTC GGT TCT GC-3'
		Reverse: 5'-GTC GAA TAG GTG TTG CTT CTC C-3'
<i>Ano2</i> 141 bp	NM_153589	Forward: 5'-TTT ATG ATT GCC CTG ACG TTC TC-3'
		Reverse: 5'-GAG GTT GAT GAT GAC TGC TGT T-3'
CCKR(A) 143-bp	NM_009827	Forward: 5'-TGT GAT GGT GGT GGC TTA CG-3'
		Reverse: 5'-CAT ATC GGC TGC TGC TGC TA-3'
CCKR(B) 142 bp	NM_007627	Forward: 5'-ACT GAG CCG ACG CCT AAG AA-3'
		Reverse: 5'-GCA GAT GAC TGT GCC GAA GA-3'
GAPDH 117-bp	NM_008084	Forward: 5'-AGC TCA CTG GCA TGG CCT TC-3'
		Reverse: 5'-TGC CTG CTT CAC CAC CTT CT-3'